In-situ Computed Tomography and Transient Dynamic Analysis of a Single-Lap Shear Test with a Composite-Metal Clinch Point

Daniel Köhler[1](✉), Richard Stephan[2], Robert Kupfer[1], Juliane Troschitz[1], Alexander Brosius[2], and Maik Gude[1]

[1] Institute of Lightweight Engineering and Polymer Technology, Technische Universität Dresden, Dresden, Germany
daniel.koehler3@tu-dresden.de

[2] Chair of Forming and Machining Processes, Technische Universität Dresden, Dresden, Germany

Abstract. Clinching is a well-established joining technology, e.g. in automotive production, because of its cost-efficiency and the ability to join different materials at low cycle times. Nowadays, a detailed quality inspection of clinch points is usually carried out ex-situ, e.g. via macroscopic examination after joining. However, only 2D-snapshots of the complex three-dimensional and time-dependent forming and damaging phenomena can be made. The closing of cracks and the resetting of elastic deformations due to unloading and specimen preparation are also disadvantageous. In contrast, the use of non-destructive in-situ testing methods enables a deeper insight into the joint deformation and failure phenomena under specific load conditions. In this paper, progressive damage is observed during the single-lap shear testing of a clinch point using in-situ computed tomography (CT) and transient dynamic analysis (TDA). The TDA can continuously monitor the characteristic dynamic response of the joint, which is sensitive to damage and process deviations. In-situ CT creates 3D images of the inner structure of the clinch point at specific process steps. In this work, the sensitivity of both testing methods to detect damage in joints with EN AW 6014 and glass fibre reinforced polypropylene (GF-PP) is evaluated. As a reference, joints with both joining partners made of aluminium alloy (EN AW 6014) are analyzed. It is shown, that TDA and in-situ CT has the potential to identify joint quality as well as critical processing times.

Keywords: Computed tomography · Active acoustic testing · Clinching

1 Introduction

Clinching is a cost-efficient joining process that allows different materials to be connected. This is particularly important in lightweight design in order to optimize the use of materials. In most cases, destructive testing methods are used for the characterization of clinch points. The preparation of a macroscopic examination is a standard method in addition to strength tests by shear-, peel- or head tensile testing [1]. A macroscopic

M. Liewald et al. (Eds.): WGP 2022, LNPE, pp. 265–275, 2023.
https://doi.org/10.1007/978-3-031-18318-8_28

examination enables the measurement of the geometric characteristics of the clinch point (undercut, neck thickness and symmetry) in a specific cross-section. Due to the resetting of elastic deformations during specimen preparation, it is possible that cracks close or cracks are not in the plane of the macroscopic examination and thus cannot be detected [2].

Using mechanical testing, maximum loads in a specific direction and the predominant failure mechanism (unbuttoning, neck breakage or a combined failure) can be determined [3]. With these methods, it is hardly possible to draw conclusions about the material flow during loading, internal damage or the failure chronology. The existing characterization possibilities can be complemented by the use of in-situ CT [4]. This imaging analysis method uses the X-ray attenuation of a test object in order to obtain a three dimensional reconstruction of the object in high resolution. For this purpose, two-dimensional radiographs of the object are created from multiple angles.

Since CT is a time-consuming procedure, it can be combined with the TDA, as described in [5]. The TDA investigates the dynamic behaviour of the clinch point by selectively introducing structure-borne sound waves and recording the response behaviour. This method offers the possibility to obtain data about the clinch point rapidly, cost-effectively and non-destructively. The method has already been applied with regard to bolted joints. Bournine et al. attempted to maximize the damping of a bolted connection while maintaining the maximum load capacity of the bolted structure [6]. Wang et al. investigated the relationship between the damping properties of a bolted joint and the preload [7]. Wolf et al. showed a change in the structure-borne sound energy dissipated in the bolted joint with varying tightening torque [8]. However, the interpretation of the data with regard to clinched joints as well as the application limits of the TDA method is still subject of ongoing research [9].

In order to evaluate the application of a combined TDA and in-situ CT, this paper examines clinched specimens consisting of an aluminium (Al) sheet (EN AW 6014) and a glass fibre reinforced polypropylene (GF-PP) sheet. To evaluate the influence of the highly damping polypropylene on the TDA, the tests were also carried out on specimens with both joining partners made of EN AW 6014.

2 Materials and Methods

2.1 Sample Preparation

Lubricated 2 mm thick aluminum sheets made of EN AW 6014-T4 (Advanz™ 6F-e170, Novelis Inc., Atlanta, USA) are used for the test specimens. The GF-PP sheets consist of glass fibre reinforced polypropylene. Both materials GF-PP [10] and EN AW 6014 [11] are typically applied in the automotive industry. For the Al-Al joints, a 0.01 mm thick tin foil is positioned between the sheets in order to enhance the visibility of the sheet-sheet interface in the CT-scan. The sheets and the foil are clinched with a punch A50100 and a die BE8012 (both from TOX PRESSOTECHNIK GmbH & Co.KG, Weingarten, Germany). Then, the specimen is solution heat-treated and artificially aged (T6) at 185 °C for 20 min. The Al-GF-PP joints are manufactured using the hotclinching method described in [12] with a process temperature of 70 °C. Here, the aluminium plate is positioned at the punch-faced side. The punch A58100 with a fillet radius of 0.25 mm

(TOX PRESSOTECHNIK) and a BE-type die with an initial anvil position of 1 mm is used. The procedure is explained in detail in [13].

The shear specimen dimensions according to ISO 12996, see Fig. 1c. In order to ensure a concentric load introduction, two shim plates are adhesively bonded onto the ends of the sheets. In contrast to the mentioned norm, the specimen width is 37 mm.

(cf. Fig. 1c) to fit the clamps. The specimen is pulled along the main axis in the in-situ CT, featuring a tensile testing machine ZwickRoell Z250 (ZwickRoell GmbH & Co. KG, Ulm, Germany) with the lower traverse moving.

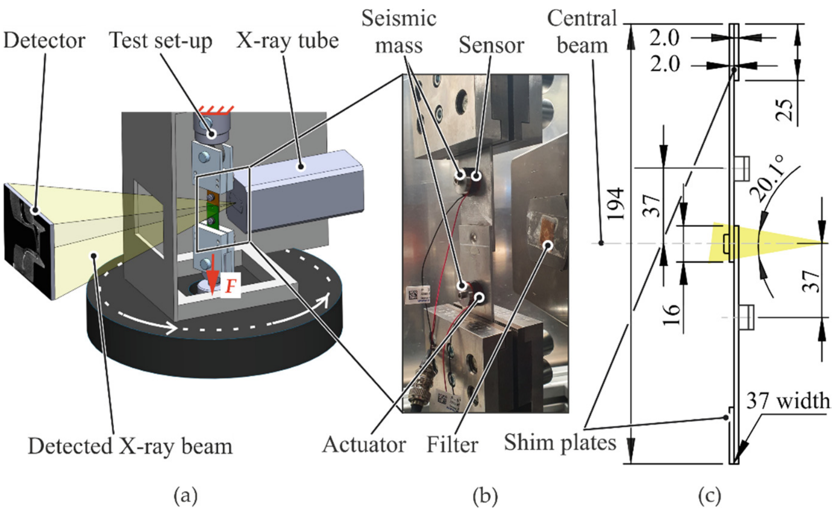

Fig. 1. Experimental setup for in-situ CT and TDA during shear testing of clinched specimens

2.2 Shear Test and CT-Setup

The CT system FCTS 160-IS (FineTec FineFocus Technologies GmbH, Garbsen, Germany) consists of the X-ray source FORE 160.01C TT (160E3 V, 1E-3 A, 80 W) and a flat panel detector (3200 × 2300 pixel, 405 × 290 mm active area).

The clinch point is CT- and TDA-scanned at six crosshead travel steps whereby the crossbeam remains at constant displacement. The crosshead travel (CHT) is selected in a way the sample displacement follows a fixed displacement step size. For the Al-Al specimens a linear relation and for the Al-GF-PP specimens a non-linear relation between crosshead travel and sample displacement is measured. A preload of 60 N is applied. The parameters for the CT scans are summarized in Table 1.

2.3 TDA Setup

To perform the TDA, structure-borne sound waves have to be introduced into the sample. This is realized by a piezoelectric ring stack actuator from the manufacturer PI Ceramic

Table 1. CT-parameter of the CT-system

Parameter	Unit	Value
Acceleration voltage	kV	150
Tube current	μA	30 (Al-Al specimen) 45 (Al-GFRP specimen)
X-ray projections	–	1440 (4 per 1°)
Exposure time	ms	625
Resolution	μm	7.58
Magnification	–	16.8
Filter	mm	0.1 (copper)

GmbH with the type designation P-016.00H. A similar piezoelectric ring stack is used to record the signal on the receiver side. In the following, these piezoelectric ring stacks are referred as actuator and sensor respectively. In order to improve the sensitivity of the sensor and to intensify the coupled sound of the actuator, both are equipped with an effective seismic mass of 9.5 g, (cf. Fig. 1b, c). The application of the seismic mass reduces the resonance frequency of the actuator and sensor from 144 kHz to pprox. 76 kHz. This improves the sensitivity and still maintains a sufficient distance from the maximum signal frequency of 22 kHz used in the test. Actuator and sensor are mounted on the specimen with a tightening torque of 1 Nm. Holes of 3.3 mm are drilled for the bolts at a distance of 37 mm from the clinch point on the respective sheet (cf. Fig. 1c). Besides mounting, the fastening also generates the compressive stress in the actuator that is necessary for dynamic operation. An analogue output of the data acquisition card NI6356 is used to excite the actuator. The alternating signal from the data acquisition card in the form of a sine with 4 V peak is converted via an analogue signal amplifier of the type HV-LE150-100-EBW from the manufacturer piezosystem jena GmbH into an excitation with 67 V peak for the actuator. The analogue output signal of the sensor passes through a first-order high-pass filter with a cut-off frequency of 147 Hz in order to reduce the interspersed influences of the surrounding electrical devices. The filtered signal is amplified by a Kistler 5018 charge amplifier and then sampled by the NI6356 using a sampling rate, which always equals eight times the excited frequency.

During the TDA, a specific frequency is always excited for a duration of two seconds. The measuring program always stores the sampled signal from the final half second of each frequency in order to process only data from the steady state. After these 2 s, the frequency to be stimulated is increased by 50 Hz. The spectrum of the TDA starts at 200 Hz and finishes at 22,000 Hz. For each excited frequency, the amplitude value is taken and added to the frequency spectrum.

3 Results

3.1 CT-Results

Figure 2 shows six CT images of Al-Al sample C04_A_CV_240_ZS_180 at different process steps of the shear test. The interface between the sheets in the clinch point area, which is highlighted by the tin foil, can be clearly seen. It also makes the undercut of the clinch point in Fig. 2a visible. The chronology of the present unbuttoning failure mechanism can be clearly traced (cf. Fig. 2c–f). There is a significant stretching of the right neck area of the punch-side sheet from Fig. 2b–f. Despite the shear between the sheets in this area, the tin foil remains free of macroscopic ruptures. However, in the left half of the images, the punch-side joining partner deforms and the bottom glides along the neck area of the die-sided joining partner. At this are the tin foil breaks. At the same time, the bottom of the punch-sided sheet is bended off the die-sided sheet, reducing the contact area between both sheets.

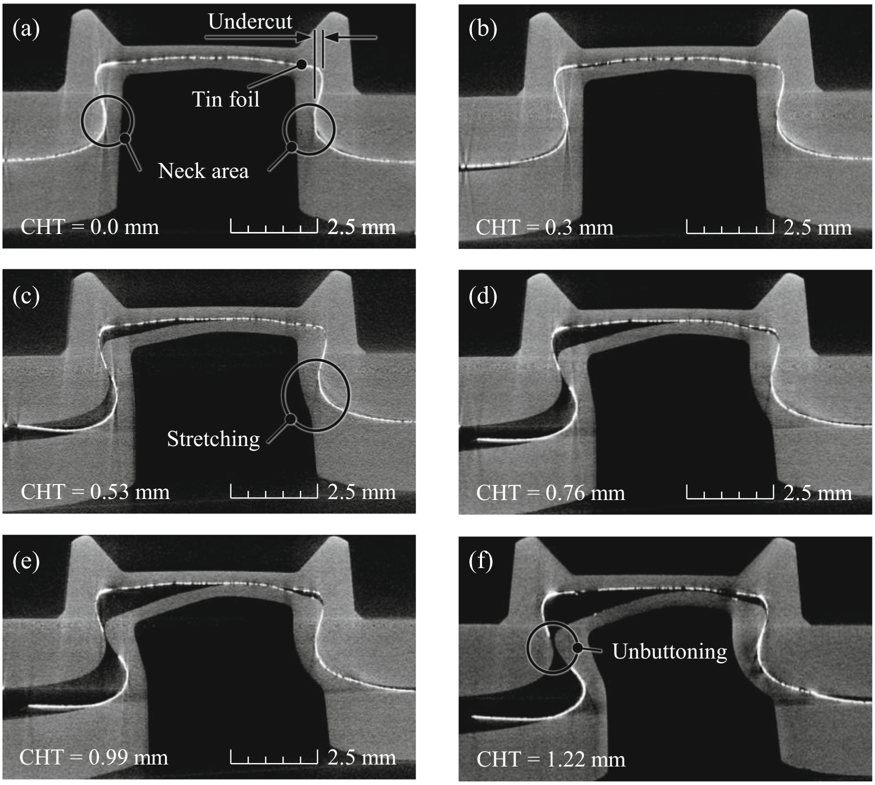

Fig. 2. CT scans of sample C04_A_CV_240_ZS_Z180 at different CHT steps from 0.0 mm (a) to 1.22 mm (f)

Figure 3 shows the CT scans of sample A01_FKVA_CV_03 during the shear tensile test on different CHT. Initially, there is a crack in the Al joining partner in the neck area visible (cf. Fig. 3a). In the FRP joining partner a thin FRP layer with lower fibre volume content remains at the bottom side of the clinching point. Additionally, there is a gap between the FRP and the Al joining partner. Despite the initial neck crack in the Al partner, the failure of the specimen is caused by unbuttoning (cf. Fig. 3f). While the Al-Al specimen was unbuttoned under strong plastic deformation of the punch-side sheet, no deformation of the Al joining partner is visible in the Al-GF-PP specimen. Instead, the bottom and neck area of the punch-side sheet increasingly press into and deforms the right clinch point shoulder of the die-side GF-PP joining partner. Thereby, the two sheets increasingly separate from each other. At the same time, the contact area on the left side of the clinching point decreases until unbuttoning results, see Fig. 3f.

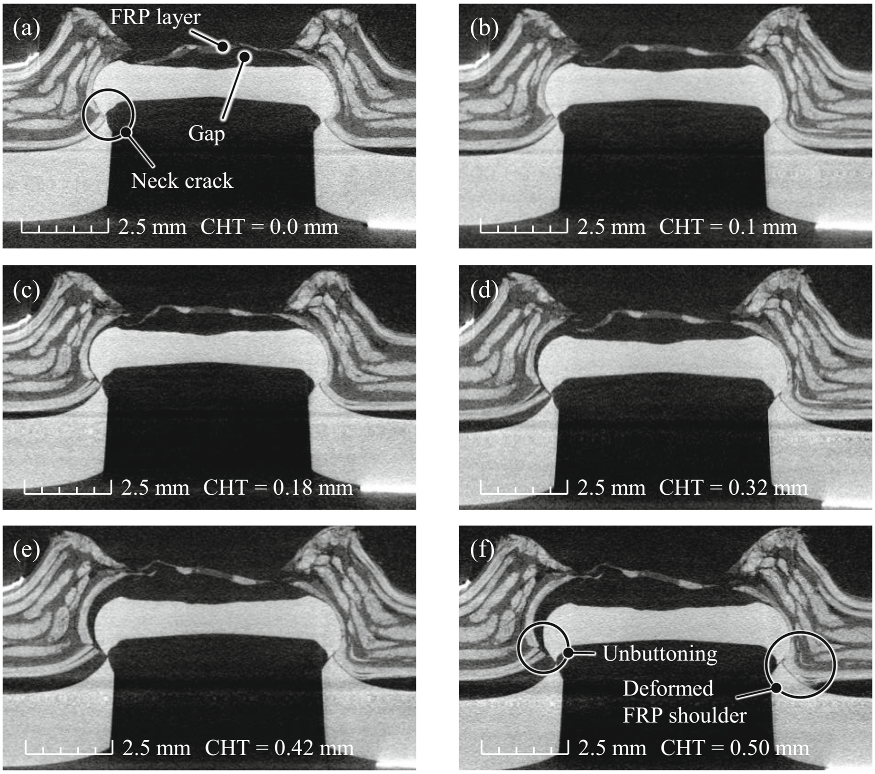

Fig. 3. CT-Scans of sample A01_FKVA_CV_03 at different CHT steps from 0.0 mm (a) to 0.5 mm (f)

3.2 Results of the Combined TDA and Single Lap Shear Test

The TDA result is a frequency spectrum of the amplified sensor signal for each measuring step. In Table 2, the TDA amplitudes are averaged at the time of achieving the mentioned test preload (60 N), i.e. before the actual shear test. In addition, the maximum force achieved in shear test is given.

Table 2. Averaged TDA amplitudes and maximum forces

No	Specimen	Material bottom plate	TDA amplitude in mV	Max. Shear force in N	Crosshead travel in mm
1	A01_FKVA_CV_01	GF-PP	79	499	0.50
2	A01_FKVA_CV_03	GF-PP	103	526	0.10
3	C04_A_CV_240_ZS_Z180	EN AW 6014	192	1972	1.22
4	C04_A_CV_238_ZS_Z180	EN AW 6014	209	1998	0.30

For both types of specimens, increasing maximum shear force will result in larger TDA amplitudes as measurement signals. The average TDA amplitudes of the Al-GF-PP specimens are about half the size of the Al-Al specimens.

In order to investigate whether the signal is sufficient to carry out a measurement on strongly damping materials, it is set in relation to the measured noise. The signal-to-noise ratio (SNR) defines the ratio of the effective value of the useful signal to the effective value of the interfering signal on a logarithmic scale using the unit dB. Four SNR graphs are shown in Fig. 4 as indicators for signal quality. The SNR graphs of all clinched joints are very similar. In order to maintain clarity, only the SNR graphs with the highest and with the lowest average SNR of both sample types are shown. All graphs show a strong increase of the SNR with increasing frequency. In the frequency range between 0 to 5 kHz the SNR of Al-GF-PP samples is mostly smaller than 10 dB. For Al-Al samples, the SNR of 10 dB is already stable at frequencies from 2 kHz. For high frequencies, the SNR increases to 80–100 dB for all samples. The largest average SNR value of Al-GF-PP samples (50.6 dB) is 2.6 dB smaller than the smallest average SNR value of Al-Al samples. For all samples, it can be noted that the SNR decreases as the shear test progresses. The selected four values also show this behaviour, as the highest average SNR values are obtained at the beginning of the test and the lowest at the end of the shear test. Because the noise is only measured once, this observation results from the average decreasing signal power at the sensor as the shear test progresses.

In Fig. 5 it can be seen, that the frequency spectra for different CHT show a very similar course. Particularly obvious is the continuous shrinking and finally disappearance of the large peak at 16.5 kHz with increasing CHT. Also noticeable is the peak shifting to smaller frequencies and shrinking at the same time, which is at 21 kHz at the beginning of the test.

Figure 6 shows four TDA frequency spectra of sample No. 3, Table 2 at different crosshead travel (CHT) steps. Overall, the changes in the frequency spectra for this Al-Al sample are less continuous than for sample No. 2. In order to achieve clarity, fewer spectra are shown than in Fig. 5. Beside the fact, that for both material combination, Al-Al and Al-GF-PP, differences in the frequency spectrum occurs, the amplitudes of both material combinations are getting larger with increasing frequency. The peaks in the spectra of sample No. 3 with a maximum of 2.3 V are significantly larger than the largest peaks of sample No. 2 with about 0.6 V. It is noticeable that both samples have

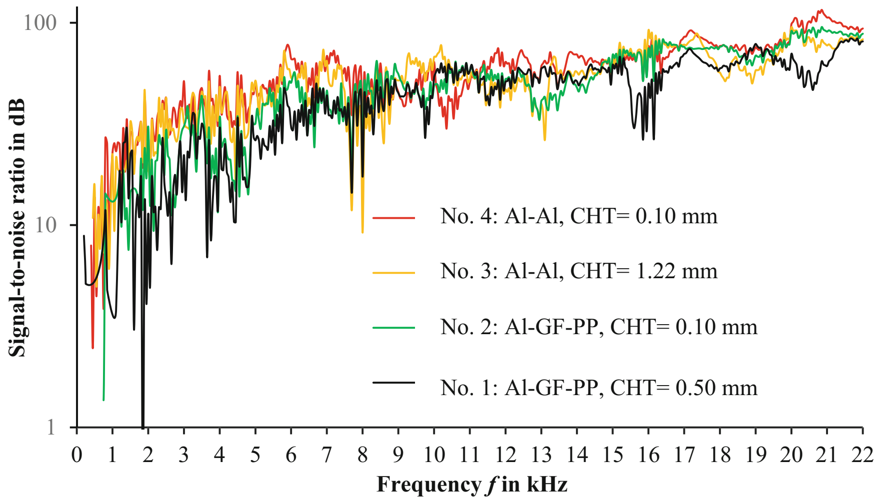

Fig. 4. Signal-to-noise ratio of different specimens

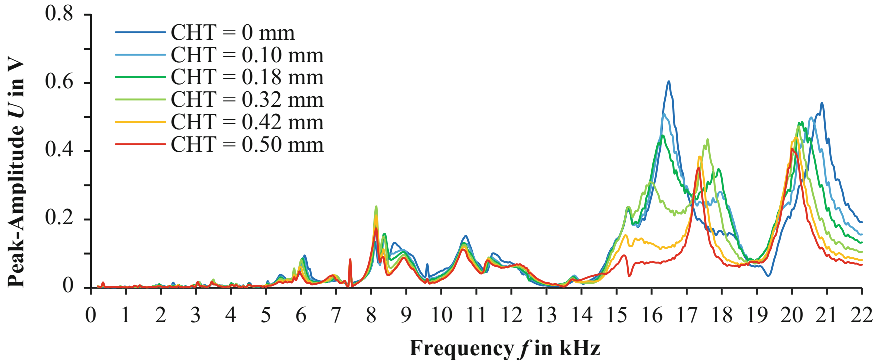

Fig. 5. Frequency spectra of the peak amplitudes of the TDA signal of the sample No. 2

their largest peak at about 16.5 kHz. However, while this peak in sample No. 2 becomes steadily smaller as the shear tensile test progresses, in sample No. 3 it also becomes smaller at first and then increases again to the original height.

4 Summary, Discussion and Conclusions

With conventional characterization methods, it is hardly possible to draw conclusions about the material flow during loading of a clinch point. Additionally, internal damage or the failure chronology remain unknown. The in-situ CT in combination with TDA has the potential to compensate these drawbacks. In this work, the feasibility of the combined measurement is investigated et al. -GF-PP. The results are compared with those from Al-Al joints.

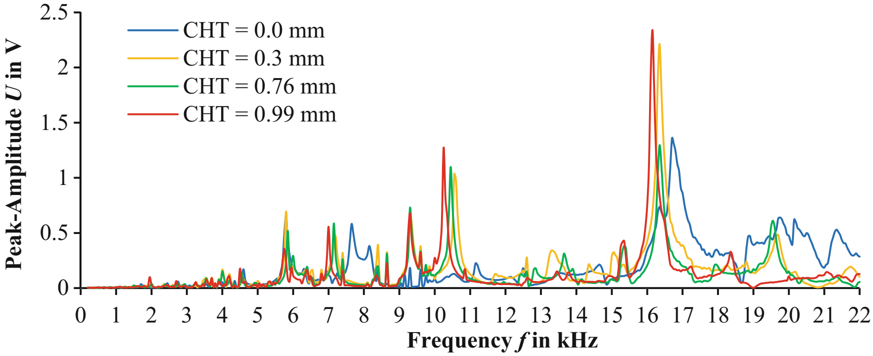

Fig. 6. Frequency spectra of the peak amplitudes of the TDA signal of sample No. 3

Using in-situ CT, the chronology of specimen failure during shear testing can be easily traced. Both types of specimens fail by unbuttoning. However, a clearly different failure development is recognizable. The Al-Al specimens fail under heavy deformation of the neck area of the punch-side sheet with a significant change in geometry. In contrast, the Al-GF-PP specimens do not show any change in the geometry of the punch-side Al sheet. Instead, the neck and head of Al sheet presses increasingly into the shoulder of the GF-PP joining partner and deforms it. This precise characterisation of the failure of the two specimens enables the conclusion of recommendations for improving of the shear strength. For the Al-Al specimens, the maximum shear force could be improved if the top sheet's unbuttoning resistance is increased. For example, this can be achieved by adapting the clinching tools' geometry resulting in an increased undercut. To improve the shear strength of the PF-PP Al composite, the strength of the GF-PP against impression would have to be improved.

In TDA, a significantly greater damping of the fibre-reinforced plastic compared to aluminium is measured. This is particularly evident in the lower amplitudes over the entire frequency range of the TDA, but also in a reduced SNR compared to the Al-Al samples. The averaged SNR for Al-GF-PP samples is 2.5–14.2 dB lower than for Al-Al samples. In principle, the noise that reaches the sensor in the form of structure-borne sound is also damped by the plastics, but other influences via airborne sound, electrical influences via induction and the noise of the measuring amplifier remain of the same magnitude with a significantly reduced signal amplitude at the same time.

TDA on Al-Al samples achieves good signal quality above 2 kHz. In the case of Al-GF-PP samples, the signal quality achieves a sufficient SNR of stable above 10 dB from 5 kHz onwards. One conclusion is that in terms of signal quality, TDA can therefore be implemented above this frequency, even with the highly damping material GF-PP.

The interpretation of the TDA data is still a subject of research. However, by combining the data with the in-situ CT, explanations for some of the observations in the TDA results can be found. So, at both samples the amplitudes decrease with increasing crosshead travel. This observation could be explained by the continuous reduction of the contact area between the joining partners, which is recognizable in both sample types (cf. Figs. 2, 3). TDA results of the Al-Al samples show less continuously and smooth changes of the TDA characteristics than the Al-GF-PP samples. This could be explained by the strong deformation of the clinch point area on the punch side (cf. Fig. 2c–f) and the resulting change in dynamic properties. The Al-GF-PP samples, on the other hand, do not show such macroscopic changes in the geometry of the joining partners. A continuous pressing of the aluminium into the reinforced plastic during joining as well as the continuously increasing sheet distance (cf. Fig. 3) is a possible explanation for the mentioned typical characteristic of the TDA signal. The continuous changes in the TDA signal during the shear test of Al-GF-PP samples could be a utilisable feature for monitoring the clinching process by TDA. It is possible that these features can be used to identify the failure characteristics during a shear test using TDA.

5 Outlook

Beside the possibility for online monitoring of the clinching process by TDA another option is the combined usage of TDA and in-situ CT. The continuous online monitoring by TDA could be used to identify a critical time during clinching, when cracks or other failure mechanisms starts. At these relevant points of interest, the joining process would be stopped and the time intensive scanning process of in-situ CT can start. Moreover, TDA could be used for other applications, such as process monitoring or the inspection of clinch joints located on structures in operation. Both applications will be investigated in future.

Acknowledgements. This research was funded by the German Research Foundation (DFG) within the project Transregional Collaborative Research Centre 285 (TRR 285) (project number 418701707), sub-project C04 (project number 426959879).

References

1. Kupfer, R., et al.: Clinching of aluminum materials—methods for the continuous characterization of process, microstructure and properties. J. Adv. Joining Process. J. Pre-Proof (2022). https://doi.org/10.1016/j.jajp.2022.100108
2. Böhm, R., et al.: A quantitative comparison of the capabilities of in situ computed tomography and conventional computed tomography for damage analysis of composites. Compos. Sci. Technol. **110**(2015), 62–68 (2015). https://doi.org/10.1016/j.compscitech.2015.01.020
3. ISO 12996:2013: Mechanical joining—destructive testing of joints—specimen dimensions and test procedure for tensile shear testing of single joints
4. Köhler, D., Kupfer, R., Troschitz, J., Gude, M.: In situ computed tomography—analysis of a single-lap shear test with clinch points. Materials **14**(8), 1859 (2021). https://doi.org/10.3390/ma14081859
5. Köhler, D., Sadeghian, B., Kupfer, R., Troschitz, J., Gude, M., Brosius, A.: A method for characterization of geometric deviations in clinch points with computed tomography and transient dynamic analysis. Key Eng. Mater. **883**, 89–96 (2021). https://doi.org/10.4028/www.scientific.net/KEM.883.89
6. Bournine, H., Wagg, J., Neild, S.A.: Vibration damping in bolted friction beam-columns. J. Sound Vib. **330**(8), 1665–1679 (2011). https://doi.org/10.1016/j.jsv.2010.10.022

7. Wang, F., Huo, L., Song, G.: A piezoelectric active sensing method for quantitative monitoring of bolt loosening using energy dissipation caused by tangential damping based on the fractal contact theory. Smart Mater. Struct. **27**(1) (2017). https://doi.org/10.1088/1361-665X/aa9a65
8. Wolf, A., Lafarge, R., Kühn, T., Brosius, A.: Experimental analysis of mechanical joints strength by means of energy dissipation. In: Proceedings of the 21st International ESAFORM Conference on Material Forming, AIP Publishing (2018). https://doi.org/10.1063/1.503488
9. Sadeghian, B., Guilleaume, C., Lafarge, R., Brosius, A.: Investigation of clinched joints—a finite element simulation of a non-destructive approach. In: Behrens, B.-A., Brosius, A., Hintze, W., Ihlenfeldt, S., Wulfsberg, J.J. (eds.) WGP 2020. LNPE, pp. 116–124. Springer, Heidelberg (2021). https://doi.org/10.1007/978-3-662-62138-7_12
10. Puri, P., Compston, P., Pantano, V.: Life cycle assessment of Australian automotive door skins. Int. J. Life Cycle Assess. **14**, 420–428 (2009). https://doi.org/10.1007/s11367-009-0103-7
11. Bhattacharya, R., Stanton, M., Dargue, I., Williams, G., Aylmore, R.: Forming limit studies on different thickness aluminium 6xxx series alloys used in automotive applications. Int.J. Mater. Form. **3**, 267–270 (2010). https://doi.org/10.1007/s12289-010-0758-4
12. Gröger, B., et al.: Clinching of thermoplastic composites and metals—a comparison of three novel joining technologies. Materials **14**(9), 2286 (2021). https://doi.org/10.3390/ma14092286
13. Vorderbrüggen, J., Gröger, R., Kupfer, R., Hoog, A., Gude, M., Meschut, G.: Phenomena of forming and failure in joining hybrid structures—experimental and numerical studies of clinching thermoplastic composites and metal. In: AIP Conference Proceedings, vol. 2113, p. 050016 (2019). https://doi.org/10.1063/1.5112580